1

Introduction

When electromagnetic waves pass through an interface between two media, the reflection angle is equal to the incidence angle, and the transmission angle follows Snell's law. So, what if one wants electromagnetic waves to have richer reflection and transmission characteristics at the interface? The answer is the artificial surface, i.e., metasurface, which is generally defined as an "artificial" two-dimensional material composed of an array of electrically small scatterers, with electromagnetic properties that cannot be found in natural media. Metasurface has been a research hotspot in many fields, such as optics, communications, radar, and antennas, in the past decade.

Figure 1.1 shows the number of publications with "metasurface" as a keyword in the core database of the Web of Science since 2000 [1]. As a comparison, we show the number of the keyword "FDTD" (finite-difference time-domain method), which is a classic and widely used computational electromagnetic algorithm and is also one of the algorithms employed in this book. It can be seen that the research on metasurface has increased rapidly in the past 10 years. Figure 1.2 shows the word frequency statistics of the titles of the accepted papers at AP-S/URSI 2024 in Italy [2], in which metasurface ranks fourth among all the keywords with a rate of 7.3%.

Before fabrication, electromagnetic simulation of the metasurface is a necessary step, which is an imitative representation of the possible response of metasurfaces in the real world. Different from the classical electromagnetic full-wave simulation problems such as waveguide transmission, antenna design, characteristic mode analysis, and radar cross-section calculation, the simulation of the metasurface is a complex electrical multiscale problem caused by the combination of the electrically small structure of meta-atoms and the electrically large array, which needs a lot of computational resources and hence limits the development of metasurface.

Therefore, this book introduces a fast simulation method for metasurfaces, i.e., the generalized sheet transition conditions (GSTC), which have become popular

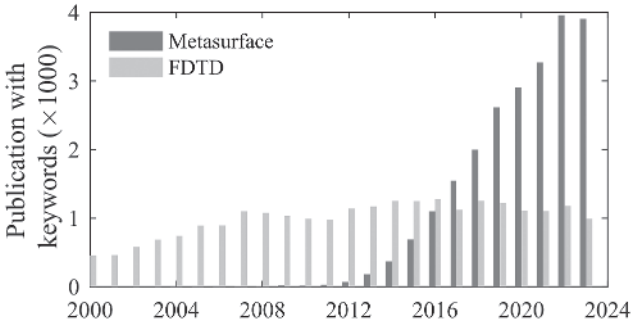

Figure 1.1 Number of publications with keywords "Metasurface" and "FDTD" in Web of Science.

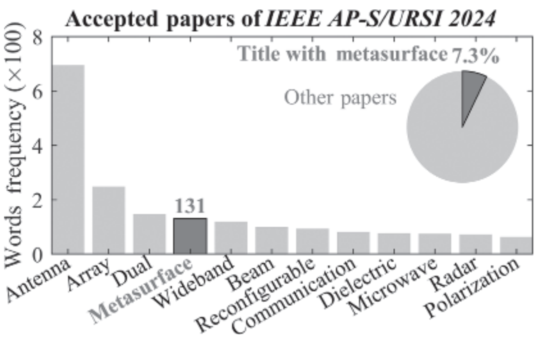

Figure 1.2 The word frequency of the titles of the accepted papers in the 2024 IEEE International Symposium on Antennas and Propagation and INC-USNC-URSI Radio Science Meeting (AP-S/URSI).

and well studied recently. Based on the homogenization theory, it uses surface parameters to replace the subwavelength structure equivalently in the full-wave simulations, avoiding the excessive computational resources of brute-force direct solving. This book provides a systematic and detailed description of how to combine GSTC with the six mainstream computational electromagnetic methods, with numerical examples. Since there is no commercial software including GSTC yet, this book is valuable in paving a new way for the fast analysis of metasurfaces.

1.1 Overview of Metasurfaces

The concept of metasurfaces emerged from the field of metamaterials, which are engineered to have properties not found in nature. Early work on metamaterials focused on three-dimensional (3-D) structures designed to manipulate electromagnetic waves, leading to the concept of negative-index materials, first theoretically proposed by Veselago in 1967 [3] and then experimentally realized by Smith in 2000 [4]. The invisibility cloak, which sounds like a magic tool from science fiction, has been successfully realized by metamaterials [5]. Since then, metamaterials have captured the interest of both researchers and the public and have found great applications in improved imaging systems, advanced telecommunications, and innovative medical devices [6].

However, metamaterials are limited by their thickness in the direction of propagation, which leads to excessive loss, and researchers need to use several times or even dozens of times the excitation power in order to obtain electromagnetic waves with the required properties. Besides, the complexity of large-scale 3-D manufacturing is another key point that hinders the wide industrial applications of metamaterials. In 2002, two groups [7, 8] proposed two-dimensional metamaterials based on the transmission line concept to decrease the loss significantly, which is the prototype of the metasurface.

Metasurfaces not only achieve similar or even superior abilities to manipulate electromagnetic waves at a surface rather than throughout a volume, but also have the advantages of easier fabrication, lower losses, and smaller physical dimensions. Over the years, metasurfaces have been applied across a large spectrum range, from radio frequency to optical regimes, enabling advanced applications such as flat lenses for focus and imaging, communication systems, and cloaking and stealth technology. Figure 1.3 depicts eight real applications with metasurfaces, including (a) metasurface-based wearable sensor, (b) antenna decoupling, (c) multicolor and 3-D holography generator, (d) orbital angular momentum (OAM) wave generator, (e) Bessel beam former, (f) polarization selector, (g) RCS reduction, and (h) conformal antenna. Functionalities have been greatly enriched to control one or more aspects of electromagnetic waves, and three typical ones are described as follows.

Amplitude Control: When electromagnetic waves impinge on a surface between two media, reflection and refraction happen, and the ratio of them depends on the refractive index contrast. Metasurface provides the possibility to manipulate the amplitudes of the reflected and transmitted waves at will. High-impedance metasurfaces not only enable high reflection but also reflect the incident plane wave in phase and suppress surface waves [17]. These unique properties are useful for applications such as low-profile directed antennas [18, 19], scattering reduction [20], and antenna decoupling [10, 21].

The concept of controlling amplitude by surface impedance also leads to the perfect absorbers and the frequency-selective surfaces [22–24]. By carefully

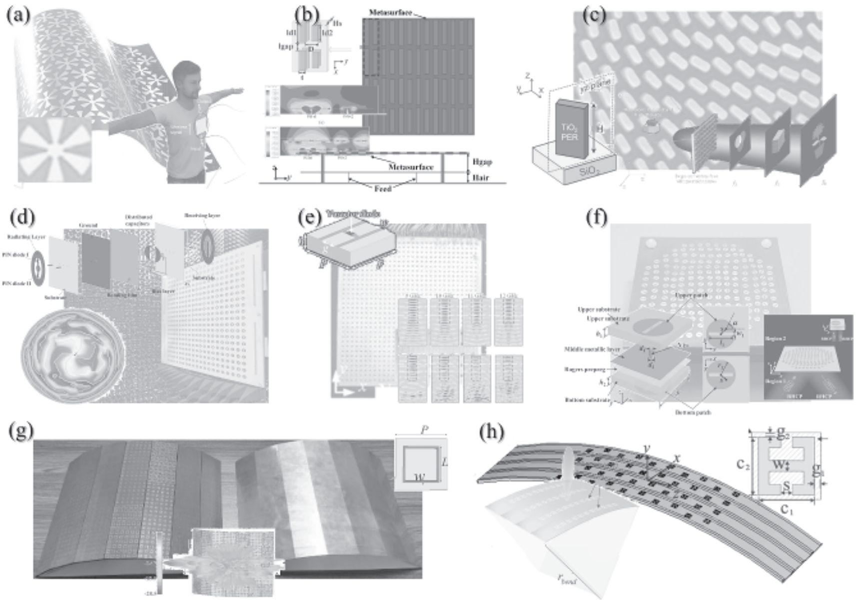

Figure 1.3 Some typical applications of metasurfaces. The figures with the gray filter are the metasurface array, the blue structures are the meta-atoms, while the orange sketches are the function of the metasurfaces. (a) Metasurface-based wearable sensor. *Source:* Chen et al. [9] / with permission of John Wiley & Sons, (b) antenna decoupling. *Source:* Liu et al. [10] / with permission of IEEE, (c) multicolor and 3-D holography generator. *Source:* Adapted from So et al. [11], (d) OAM generator. *Source:* Adapted from Bai et al. [12], (e) Bessel beam former. *Source:* Adapted from Feng et al. [13], (f) polarization selector. *Source:* Adapted from Yang et al. [14], (g) RCS reduction. *Source:* Adapted from Wang et al. [15] / with permission of IEEE, and (h) conformal antenna. *Source:* Adapted from Yoo and Smith [16].

designing the electric and/or magnetic impedances of the structured surfaces, they can perform functions such as energy harvesting [25, 26], sensing [9, 27], and spectral and spatial filtering [28].

Wavefront Control: Wavefront control is typically achieved through phase manipulation. In traditional surfaces, this is severely limited by the inherent properties of the material. Fortunately, metasurfaces offer the capability to introduce phase discontinuities by specifically designing and arranging meta-atoms, allowing for flexible control of electromagnetic wavefront [29]. Various phase strategies are available, including the propagation phase, geometric phase, and resonance phase [30]. By employing these design techniques, meta-atoms with 2π phase coverage can be engineered, and metasurfaces with controllable phase profiles can be constructed to achieve a range of advanced functionalities, like beam shaping and holographic projection [11, 31]. Consequently, metasurfaces have found widespread applications from microwave to optical wavelengths. In the microwave domain, metasurfaces are frequently used for beam focusing to enhance antenna gain and transmission efficiency [32]. In the terahertz and optical bands, in addition to beam focusing, metasurfaces are also engineered to generate specialized beams, such as vortex beams [33] and Bessel beams [13].

Polarization Control: Traditional polarization controllers rely on the anisotropy of natural materials, inherently giving rise to the drawbacks of bulky size, narrow-band operation, and limited functionality. Metasurfaces precisely control the polarization of electromagnetic waves on ultrathin thicknesses by anisotropic meta-atoms, e.g., T-, C-, and L-shaped structures and their different spatial positions and orientations [34].

For instance, by designing metal H-shaped structures or the metal cut wires as top resonators of the metal-insulator-metal (MIM) configuration, the polarization states of reflected waves can be manipulated and experimentally implemented in the microwave [35], terahertz [36], and optical frequency bands [37], with their polarization conversion ratios (PCR) approaching 100%. Due to the low conversion efficiencies, controls on transmitted waves would be a little bit difficult. Despite this, the T-shaped meta-atoms made a metasurface to perform as a quarter-wave plate (QWP) with a ~50% efficiency and a broad bandwidth across the visible to near-infrared range [38], while chiral metasurfaces provide the ability to improve the PCR and the working efficiency [39, 40]. The latter can even enhance chirality and chiral near-fields to stimulate biosensing for chiral molecules. Also recently, bifunctional or multifunctional metasurfaces involving polarization manipulation have promoted themselves to real-world applications in wireless communication and detection [14].

As research develops on the theory and mechanism, design, numerical simulation, physical implementation, and experimental measurement, the field of the metasurface is growing prosperously to profoundly revolutionize electromagnetic science [41, 42].

1.2 Computational Electromagnetic Methods

Some solutions can be obtained analytically, such as the plane wave solution in vacuum based on the rectangular coordinate system, the Bessel function solution in vacuum based on a cylindrical coordinate system, and the transverse electric (TE) and transverse magnetic (TM) mode solutions in a waveguide.

These are the analytical solutions of Maxwell's equations under corresponding boundary conditions. However, most practical engineering problems have no analytical solutions because of their irregular geometries. Hence, researchers use numerical methods to find approximate solutions to these problems. Based on numerical analysis and computer technology, the discipline of researching numerical solutions is called computational electromagnetics (CEM). Since its development in the early 1960s, CEM has been widely used in radar, antenna, microwave, circuit, electronic and nanodevices, biomedicine, electromagnetic imaging, and so on [43, 44].

There are two main types of CEM methods: high-frequency approximation methods and full-wave methods. The high-frequency approximation method is based on the optical description of high-frequency electromagnetic waves, and the size of the problem is usually much larger than the working wavelength. This category includes the basic geometrical optics (GO) method and physical optics (PO) method, and the methods incorporating diffraction theory, such as geometrical theory of diffraction (GTD) method and physical theory of diffraction (PTD) method. Subsequent developments include the unified theory of diffraction (UTD) and the shooting and bouncing ray (SBR) method. Since these high-frequency approximation methods are rarely used in metasurface simulation, they will not be covered in this book. The full-wave methods, which constitute the main content of this book, are based on strict numerical solutions of Maxwell's equations, Helmholtz equations, or various integral equations in the frequency domain or time domain. According to the different mathematical properties of the governing equations, they can be subdivided into two types of numerical full-wave methods, i.e., the partial differential equations (PDE)-based method and the integral equations (IE)-based method. Full-wave models extensively make use of symmetry, infinity, and periodicity, and solve for reduced dimensionality from 3-D problems to two-dimensional (2-D) ones or even one-dimensional (1-D) ones, which will be often seen in this book. The six numerical CEM methods introduced in the following chapters are

1) Finite-difference frequency-domain (FDFD) method [45]
2) Finite element method (FEM) [46]
3) Spectral element method (SEM) [47]
4) Boundary element method (BEM) [48]
5) Finite-difference time-domain (FDTD) method [49]
6) Discontinuous Galerkin time-domain (DGTD) method [50]

where methods 1, 2, 3, 5, and 6 are PDE methods, and method 4 is the IE method. The control equations of PDE methods, i.e., Maxwell's equations, are written as

$$\nabla \times \mathbf{E} = -\frac{\partial \mathbf{B}}{\partial t} \tag{1.1.a}$$

$$\nabla \times \mathbf{H} = \frac{\partial \mathbf{D}}{\partial t} + \mathbf{J} \tag{1.1.b}$$

$$\nabla \cdot \mathbf{D} = \rho \tag{1.1.c}$$

$$\nabla \cdot \mathbf{B} = 0 \tag{1.1.d}$$

where the field quantities **E**, **H**, **D**, and **B** are electric field intensity, magnetic field intensity, electric flux density, and magnetic flux density. The source terms **J** and ρ are volume current density and free volume charge density. The IE method is based on the equivalence principle, which requires integrating the equivalent electric current $\mathbf{J}_s$ and magnetic current $\mathbf{K}_s$ on the metasurface to solve the field response. The control equations are written as

$$\mathbf{E} = -\mathrm{j}kZ \int \left[\mathbf{J}_s + \frac{1}{k^2}\nabla(\nabla \cdot \mathbf{J}_s)\right] G\mathrm{d}r_s + \int \mathbf{K}_s \times \nabla G\mathrm{d}r_s \tag{1.2.a}$$

$$\mathbf{H} = -\mathrm{j}\frac{k}{Z} \int \left[\mathbf{K}_s + \frac{1}{k^2}\nabla(\nabla \cdot \mathbf{K}_s)\right] G\mathrm{d}r_s - \int \mathbf{J}_s \times \nabla G\mathrm{d}r_s \tag{1.2.b}$$

where Z, k, and G denote the wave impedance, wave number, and the Green's function. In metasurface simulations, when we want to know the macroscopic response of a metasurface under excitations such as linearly polarized plane waves, we need to identify a region around the geometry of this metasurface and discretize this region with grids, and this region is called the computational domain, and the discretization is called meshing. The PDE-based method also imposes a truncation condition on the boundary of the computational domain to mimic an infinite open space outside the computational region. Methods 1 and 5 use regular square grids, called structured mesh, while methods 2, 3, 4, and 6 support unstructured grids, such as tetrahedrons and hexahedrons.[1] The unstructured grids are geometrically flexible and suitable for metasurfaces with complex geometric structures and curved arrays. In each grid, whether to use a known base, such as a polynomial series, to approximate the solution is also one of the differences between methods 1, 5 and 2, 3, 4, 6. This base is called the basis function, and the highest power series that the basis function can represent is its order. The advantage of the basis function is that the precision can be improved by setting the order of basis functions, which provides a method to improve the precision in addition to enhancing the meshing density. The number of the basis functions is referred to as the degrees of freedom (DoFs). Finally, according to whether the fields are time-dependent or time-harmonic, the methods can be divided into frequency-domain methods and time-domain methods, which is also the reason for the division of Chapters 3 and 4 of this

1 Of course, the FD method also has related research using unstructured grids, but in this book, we only discuss the basic form of each algorithm.

Table 1.1 Simple comparison of the six numerical CEM methods introduced in this book.

	FDFD	FEM (SEM)	BEM	FDTD	DGTD
Controlling equation	PDE	PDE	IE	PDE	PDE
Grid type	Structured	Unstructured	Unstructured	Structured	Unstructured
Basis function	×	√	√	×	√
Working domain	Frequency	Frequency	Frequency	Time	Time

book. The frequency-domain methods 1, 2, 3, and 4 obtain the steady-state solution under harmonic illumination, which is suitable for single-frequency analysis, while the time-domain methods 5 and 6 obtain the transient solution, which is suitable for broadband analysis. To summarize, Table 1.1 gives a simple comparison of the six methods used in this book.

In addition to the above full-wave methods, there are other full-wave methods for metasurface analysis, such as the Cagniard-De Hoop technique [51], but until the publication of this book, there is no published work combining them with GSTC, so they will not be covered in this book.

1.3 Layout of This Book

Chapter 2 introduces the GSTC theory. Beginning with the asymptotic analysis of Maxwell's equations, we introduce the concept of using homogenization to replace electrically small structures and the related basic concepts of electromagnetism, and we also introduce some classical boundary conditions. Then, we derive the expression of GSTC rigorously from mathematics and electromagnetism and compare it with the traditional boundary conditions. Finally, we give the methods to determine the equivalent parameters of GSTC, i.e., the surface susceptibility tensor.

Chapter 3 introduces the FDFD, FEM, SEM, and IE (BEM) methods. All these methods are developed in the following order, i.e., basic theories (especially the parts related to GSTC), the strategies for integrating GSTC in their basic framework, and simulation examples of metasurface using the incorporated methods.

Chapter 4 introduces the FDTD and DGTD methods and follows the same way as Chapter 3.

Chapter 5 presents an overview of this book and discusses the state of the art in metasurface fast simulation, and finally closes with some remarks on future challenges.

References

1 Clarivate, Journal Citation Reports, 2024. https://jcr.clarivate.com/ Dec 10, 2024.

2 APS-URSI 2024, List of Accepted Papers, 2024. https://2024.apsursi.org/papers/accepted_papers.php Dec 10, 2024.

3 V. G. Veselago, "The electrodynamics of substances with simultaneously negative values of ε and μ," *Sov. Phys. Uspekhi*, vol. 10, no. 4, p. 509, 1968.

4 D. R. Smith, W. J. Padilla, D. Vier, S. C. Nemat-Nasser, and S. Schultz, "Composite medium with simultaneously negative permeability and permittivity," *Phys. Rev. Lett.*, vol. 84, no. 18, p. 4184, 2000.

5 D. Schurig *et al.*, "Metamaterial electromagnetic cloak at microwave frequencies," *Science*, vol. 314, no. 5801, pp. 977–980, 2006.

6 J. B. Pendry, D. Schurig, and D. R. Smith, "Controlling electromagnetic fields," *Science*, vol. 312, no. 5781, pp. 1780–1782, 2006.

7 A. Grbic and G. V. Eleftheriades, "Experimental verification of backward-wave radiation from a negative refractive index metamaterial," *J. Appl. Phys.*, vol. 92, no. 10, pp. 5930–5935, 2002.

8 C. Caloz, H. Okabe, T. Iwai, and T. Itoh, "Transmission line approach of left-handed (LH) materials," in *Proc. USNC/URSI National Radio Science Meeting*, vol. 1. San Antonio, TX, June 2002, p. 39.

9 L. Chen *et al.*, "Flexible and robust metasurface-based wearable sensor for intelligent human monitoring," *Adv. Mater.*, e14150, Dec. 2025.

10 F. Liu, J. Guo, L. Zhao, G.-L. Huang, Y. Li, and Y. Yin, "Dual-band metasurface-based decoupling method for two closely packed dual-band antennas," *IEEE Trans. Antennas Propag.*, vol. 68, no. 1, pp. 552–557, Jan. 2020, doi: 10.1109/TAP.2019.2940316.

11 S. So *et al.*, "Multicolor and 3D holography generated by inverse-designed single-cell metasurfaces," *Adv. Mater.*, vol. 35, no. 17, p. 2208520, 2023.

12 X. Bai *et al.*, "High-efficiency transmissive programmable metasurface for multimode OAM generation," *Adv. Opt. Mater.*, vol. 8, no. 17, p. 2000570, 2020.

13 R. Feng *et al.*, "Flexible manipulation of bessel-like beams with a reconfigurable metasurface," *Adv. Opt. Mater.*, vol. 8, no. 23, p. 2001084, 2020.

14 W. Yang *et al.*, "Polarization-selective bifunctional metasurface for high-efficiency millimeter-wave folded transmitarray antenna with circular polarization," *IEEE Trans. Antennas Propag.*, vol. 70, no. 9, pp. 8184–8194, 2022.

15 Y. Wang, J. Su, Z. Li, Q. Guo, and J. Song, "A prismatic conformal metasurface for radar cross-sectional reduction," *IEEE Antennas Wirel. Propag. Lett.*, vol. 19, no. 4, pp. 631–635, Apr. 2020, doi: 10.1109/LAWP.2020.2974018.

16 I. Yoo and D. R. Smith, “Design of conformal array of rectangular waveguide-fed metasurfaces,” *IEEE Trans. Antennas Propag.*, vol. 70, no. 7, pp. 6060–6065, Jul. 2022, doi: 10.1109/TAP.2022.3140822.

17 D. Sievenpiper, L. Zhang, R. F. J. Broas, N. G. Alexopolous, and E. Yablonovitch, “High-impedance electromagnetic surfaces with a forbidden frequency band,” *IEEE Trans. Microwave Theory Tech.*, vol. 47, no. 11, pp. 2059–2074, 1999.

18 J. Kim and Y. Rahmat-Samii, “Low-profile loop antenna above EBG structure,” in *2005 IEEE APS Int. Symp.*, 2005, vol. 2A. IEEE, pp. 570–573.

19 A. P. Feresidis, G. Goussetis, S. Wang, and J. C. Vardaxoglou, “Artificial magnetic conductor surfaces and their application to low-profile high-gain planar antennas,” *IEEE Trans. Antennas Propag.*, vol. 53, no. 1, pp. 209–215, 2005.

20 D. F. Sievenpiper, “Nonlinear grounded metasurfaces for suppression of high-power pulsed RF currents,” *IEEE Antennas Wirel. Propag. Lett.*, vol. 10, pp. 1516–1519, 2011.

21 R. F. J. Broas, D. F. Sievenpiper, and E. Yablonovitch, “An application of high-impedance ground planes to phased array antennas,” *IEEE Trans. Antennas Propag.*, vol. 53, no. 4, pp. 1377–1381, 2005.

22 Y. Ra’di, C. R. Simovski, and S. A. Tretyakov, “Thin perfect absorbers for electromagnetic waves: Theory, design, and realizations,” *Phys. Rev. Appl.*, vol. 3, no. 3, 037001, 2015.

23 B. A. Munk, *Frequency Selective Surfaces: Theory and Design*. John Wiley & Sons, 2005.

24 N. Engheta, “Thin absorbing screens using metamaterial surfaces,” in *IEEE APS Int. Symp. (IEEE Cat. No. 02CH37313)*, 2002, vol. 2. IEEE, pp. 392–395.

25 E. Cortés *et al.*, “Optical metasurfaces for energy conversion,” *Chem. Rev.*, vol. 122, no. 19, pp. 15082–15176, 2022.

26 B. Alavikia, T. S. Almoneef, and O. M. Ramahi, “Electromagnetic energy harvesting using complementary split-ring resonators,” *Appl. Phys. Lett.*, vol. 104, no. 16, 163903, 2014.

27 N. Liu, M. Mesch, T. Weiss, M. Hentschel, and H. Giessen, “Infrared perfect absorber and its application as plasmonic sensor,” *Nano Lett.*, vol. 10, no. 7, pp. 2342–2348, 2010.

28 K. Sarabandi and N. Behdad, “A frequency selective surface with miniaturized elements,” *IEEE Trans. Antennas Propag.*, vol. 55, no. 5, pp. 1239–1245, 2007.

29 N. Yu and F. Capasso, “Flat optics with designer metasurfaces,” *Nat. Mater.*, vol. 13, no. 2, pp. 139–150, 2014.

30 S. Chen, Z. Li, Y. Zhang, H. Cheng, and J. Tian, “Phase manipulation of electromagnetic waves with metasurfaces and its applications in nanophotonics,” *Adv. Opt. Mater.*, vol. 6, no. 13, p. 1800104, 2018.

31 H. Sroor *et al.*, “High-purity orbital angular momentum states from a visible metasurface laser,” *Nat. Photonics*, vol. 14, no. 8, pp. 498–503, 2020.

32 Z. N. Chen *et al.*, “Microwave metalens antennas,” *Proc. IEEE*, vol. 111, no. 8, pp. 978–1010, 2023.

33 Q. Zhou *et al.*, “Generation of perfect vortex beams by dielectric geometric metasurface for visible light,” *Laser Photonics Rev.*, vol. 15, no. 12, p. 2100390, 2021.

34 A. Arbabi, Y. Horie, M. Bagheri, and A. Faraon, “Dielectric metasurfaces for complete control of phase and polarization with subwavelength spatial resolution and high transmission,” *Nat. Nanotechnol.*, vol. 10, no. 11, pp. 937–943, 2015.

35 J. Hao *et al.*, “Manipulating electromagnetic wave polarizations by anisotropic metamaterials,” *Phys. Rev. Lett.*, vol. 99, no. 6, 063908, 2007.

36 N. K. Grady *et al.*, “Terahertz metamaterials for linear polarization conversion and anomalous refraction,” *Science*, vol. 340, no. 6138, pp. 1304–1307, 2013.

37 J. Hao *et al.*, “Optical metamaterial for polarization control,” *Phys. Rev. A*, vol. 80, no. 2, 023807, 2009.

38 Y. Zhao and A. Alù, “Tailoring the dispersion of plasmonic nanorods to realize broadband optical meta-waveplates,” *Nano Lett.*, vol. 13, no. 3, pp. 1086–1091, 2013.

39 T. Q. Li *et al.*, “Magnetic resonance hybridization and optical activity of microwaves in a chiral metamaterial,” *Appl. Phys. Lett.*, vol. 92, no. 13, 131111, 2008.

40 A. Basiri *et al.*, “Nature-inspired chiral metasurfaces for circular polarization detection and full-Stokes polarimetric measurements,” *Light Sci. Appl.*, vol. 8, no. 1, p. 78, 2019.

41 S. Maci, “Electromagnetic metamaterials and metasurfaces: A historical journey,” *IEEE Antennas Propag. Mag.*, vol. 66, no. 3, pp. 84–101, 2024.

42 A. I. Kuznetsov *et al.*, “Roadmap for optical metasurfaces,” *ACS Photon.*, vol. 11, no. 3, pp. 816–865, 2024.

43 Q. Ren, S. Yan, and A. Z. Elsherbeni, *Advances in Time-Domain Computational Electromagnetic Methods*. Wiley, 2022.

44 X. Q. Sheng and W. Song, *Essentials of Computational Electromagnetics*. Singapore: Wiley, 2012.

45 W. Shin, “3D Finite-Difference Frequency-Domain Method for Plasmonics and Nanophotonics,” Ph.D., Stanford, CA, 2013. Accessed: Oct. 06, 2022.

46 J.-M. Jin, *The Finite Element Method in Electromagnetics*, 3rd ed. Hoboken, NJ: John Wiley & Sons Inc, 2014.

47 J. H. Lee, T. Xiao, and Q. H. Liu, “A 3-D spectral-element method using mixed-order curl conforming vector basis functions for electromagnetic fields,” *IEEE Trans. Microw. Theory Tech.*, vol. 54, no. 1, pp. 437–444, 2006.

48 R. F. Harrington, *Time-Harmonic Electromagnetic Fields*. IEEE, 2001. https://doi.org/10.1109/9780470546710.

49 S. D. Gedney, "Introduction to the finite-difference time-domain (FDTD) Method for electromagnetics," *Synth. Lect. Comput. Electromagn.*, vol. 6, 2011, doi: 10.2200/S00316ED1V01Y201012CEM027. Accessed: Jun. 14, 2022.

50 J. Álvarez González, *A Discontinuous Galerkin Finite Element Method for the Time-Domain Solution of Maxwell Equations*. Universidad de Granada, 2014. Accessed: Sep. 07, 2023.

51 M. Štumpf, *Metasurface Electromagnetics: The Cagniard-DeHoop time-domain approach*. London: SciTech Publishing, 2022.